REFERENCE

IC/94/354

INTERNATIONAL CENTRE FOR THEORETICAL PHYSICS

THEORETICAL DEVELOPMENT OF ATOMIC STRUCTURE: PAST, PRESENT AND FUTURE

S.N. Tiwary

INTERNATIONAL ATOMIC ENERGY AGENCY

UNITED NATIONS EDUCATIONAL, SCIENTIFIC AND CULTURAL ORGANIZATION

MIRAMARE-TRIESTE

IC/94/354

International Atomic Energy Agency
and
United Nations Educational Scientific and Cultural Organization
INTERNATIONAL CENTRE FOR THEORETICAL PHYSICS

THEORETICAL DEVELOPMENT OF ATOMIC STRUCTURE: PAST, PRESENT AND FUTURE[1]

S. N. Tiwary[2]
International Centre for Theoretical Physics, Trieste, Italy.

ABSTRACT

Theoretical development of atomic structure is briefly discussed. The role of correlation, relativity, quantum electrodynamic (QED), finite nuclear size (FNS) and parity nonconservation (PNC) in high precision theoretical investigation of properties of atomic and ionic systems is demonstrated. At present, we do not have a comprehensive and practical atomic structure theory which accounts all these physical effects on an equal footing. Suggestions are made for future directions.

MIRAMARE – TRIESTE

November 1994

[1]A part of this work was done while the author was Research Director and Professor, CNRS Laboratory, University of Paris-Sud, Paris and Observatoire de Paris, Meudon, Paris, France.

[2]Permanent address: Department of Physics, L.S. College, BRA Bihar University, Muzaffarpur, India.

1 Introduction

The beginning of nonrelativistic electronic structure theory can be traced back to *Bohr*[1] theory of hydrogen atom based on *Rutherford*[2] nuclear atom model and *Planck*[3] quantum idea. It is well known that the Bohr semi-classical theory is not adequate to describe the properties of many-electron systems. *Schroedinger*[4] developed the wave mechanics based on the *DeBroglie*[5] matter wave idea and *Heisenberg*[6] developed the matrix mechanics. Very shortly after the publication of the basic ideas of quantum mechanics, a general method for the determination of atomic structure was developed by *Hartree*[7]. Soon after the introduction of the Hartree model, *Fock*[8] observed that the total wave function suggested by Hartree does not have the symmetry requirement by the quantum mechanics. According to the quantum mechanics, the total wave function of a fermion system must be antisymmetry. The Hartree wave function does not satisfy the antisymmetric principle. In order to remedy this shortcoming of the theory, Fock suggested that the total wave function should be written in a determinantal form, i.e., into a form which satisfies the Pauli exclusion principle exactly. Fock has also shown that such a wave function leads to equations different from Hartree equations. *Slater*[9] derived the Hartree-Fock equation and simplified it for computation. The Hartree-Fock (HF) wave function does not include the correlation which plays an extremely important role to obtain accurate results. Several methods have been developed to incorporate electronic correlation in the atomic structure theories. Many-body perturbation *theory*[10–11] (MBPT) was introduced in atomic physics by *Kelly*[12] and provides a convenient diagrammatic form for dealing the many-electron problem. March et *al*[13] have described the many-body problem in details. However, only correlation is not adequate to explain the high precision experimental data. Inclusion of relativity is indispensable for obtaining reliable results. correlation and relativity is neither separable nor additive. They are highly coupled. Consequently, these two effects must be treated on an equal footing.

The beginning of relativistic electronic structure theory can be traced back to *Sommerfeld*[14], who combined the *Einstein*[15] theory of special relativity with the Bohr theory of hydrogen atom to treat atomic spectra and *structure*[16–17]. But the Sommerfeld theory does not obey the Lorentz invariance which is violation of the basic principle of relativity. Klein-Gordan tried to generalize the Schroedinger equation to include the relativistic effect. The Klein-Gordan equation does not follow the Lorentz invariance. *Darwin*[18] also attempted to include relativistic effect but could not succeed. *Dirac*[19] proposed the fully Lorentz invariant relativistic theory. Soon after Dirac proposed his relativistic theory of electrons and *Breit*[20] followed by deriving the Breit interaction, *Swirles*[21] tried to extend the nonrelativistic Hartree-Fock method to include relativistic effects by using the Dirac (one-electron Hamiltonian) instead of the non- relativistic one. This and subsequent ef-

forts to develop a relativistic self-consistent field (RSCF) method were stymed by the awesome computational requirements, far beyond capability at that time. Until powerful computers became available in the sixties, most relativistic calculations were limited to using the Pauli or similar approximations with nonrelativistic wave functions for atoms and ions with a small number of bound electrons.

Light emitted by ions in astrophysical and laboratory plasmas have long been used to diagnose plasma conditions. In the seventies, precise knowledge of wavelengths, transition probabilities and collision cross sections of highly charged impurities ions in tokamak plasma became critical when plasma modelling indicated that such impurities would drain energy by radiation.

A relativistic wave equation, which consists of the sum of one-electron Hamiltonian and two electrons interactions such as Coulomb interaction, has in principle an infinite number of solutions for a given total energy. This could happen if some electrons are in positive energy states and other electrons in negative energy states, with the total energy the same as that for all electrons in bound states. This mathematical dilemma known as the Brown-*Ravenhall*[22] disease, is formally avoided by introducing a projection operator in the relativistic Hamiltonian to prohibit electrons from occupying any negative energy states.

Another difficulty with the Hamiltonian is that the Breit interaction which is correction to the Coulomb electron-electron repulsive interaction, is only the first order correction. The Pauli form of Breit interaction has also been widely used to see the effect of relativity. In the language of Feynman diagrams, it represents the lowest order diagram. Much work is needed to include higher order corrections to the Breit interaction.

Dirac Hamiltonian with all corrections mentioned above cannot explain the Lamb shift. Quantum electrodynamic correction is needed. There is no simple operator for quantum electrodynamic as yet.

Relativistic calculations require much more computational effort than corresponding nonrelativistic calculations because (1) relativistic wave functions have large and small components, (2) there are two different J for each orbital angular momentum l except for s orbital, and (3) the jj coupling needed in a relativistic formulation introduces far more configurations than the LS coupling.

Most theoretical methods that are effective in calculations of high quality high-precision nonrelativistic wave functions can be converted to a relativistic form which uses the Dirac equation as the starting point. For instance, the Hartree-Fock theory and the many-body perturbation theory (MBPT) have been successfully adapted to work with the Dirac equation. These adaptations are known as the Dirac-Fock theory and the relativistic MBPT, respectively. Although, there are other, similar relativistic methods, these two methods or their variations are most flexible and likely to become methods of choice in

the future.

One notable omission in successful nonrelativistic methods adapted for a fully relativistic treatment is the *Hylleraas*[23] method which contains r_{12} variables directly in the wave functions and does not assume an independent particle model. The use of such a correlated wave function, however, raises another conceptual difficulty in developing a relativistic version. The 4-dimensional Dirac matrices α and β, are defined for one electron. In principle, these matrices become 4^N-dimensional matrices for an N-electron atom, requiring a 4^N-component correlated wave function. However, it is impractical to use this type of relativistic wave function for atoms with more than a few bound electrons. Also, since there is no specific one-electron energy associated with each electron in a Hylleraas type wave function, it is difficult to tell whether any of the electrons are in negative-energy states. Indeed, we may find an acute case of the Brown- Ravenhall disease when we try to convert the Hylleraas method to a fully relativistic form, in addition to the obvious numerical complications in dealing with a 4^N-component wave function.

To extend the Hartree-Fock or similar SCF methods into the Dirac-Fock method, one usually adopts a multiconfiguration approach because many simple nonrelativistic configurations become complex in a relativistic coupling scheme. For instance, the $2p^2$ (carbon-like) configuration in nonrelativistic notation becomes three relativistic configurations, $2p_{1/2}^2$, $2p_{1/2}2p_{3/2}$ and $2p_{3/2}^2$.

There are two different numerical schemes to implement a multiconfiguration calculation. In the first scheme, orbitals are calculated based on some common Hamiltonian or effective potential, and then their mixing coefficients are determined by a variational method while keeping the orbitals frozen. While this method is numerically stable, it requires a large number of normally unoccupied orbitals (correlation orbitals) to be effective. The second scheme is to select a small number of correlation orbitals and vary both the orbitals and mixing coefficients by a variational method. This method leads to compact total wave function with small number of correction orbitals. However, the method tends to become numerically unstable if too many correlation orbitals are included. We shall refer to the first scheme as the configuration interaction (CI) and the second scheme as the multiconfiguration Hartree-Fock (MCHF) or Dirac-Fock (MCDF) method.

The MCHF method is one of the most powerful nonrelativistic methods to account for correlation effects in a complex atoms. The necessity to use a multiconfiguration formalism in relativistic calculations is actually a blessing in disguise because the MCDF method will allow us to account for both relativistic and correlation effects.

As mentioned earlier, a projection operator is needed to prevent a relativistic solution involving pairs of electrons in positive- and negative -energy continua. Projection operators are usually formed from eigenfunctions of the wave equation to be solved, i.e., we must know the answer before we can form such an operator. Besides, we need all eigen-

functions to construct a projection operator. This necessarily forces us to look for a set of solutions based on a practical Hamiltonian for which a complete set of eigenfunctions can be generated.

Mittleman[24] has claimed that using the Dirac-Fock method is equivalent to using an appropriate projection operator. Normally, a projection operator constructed from one set of eigenfunctions will not be the correct projection operator for solutions of another wave equation. Mittleman claim of a special status for the Dirac-Fock method should be reexamined to see if his argument can be extended to a wider class of Dirac-Fock wave functions than he originally treated. For instance, it is unlikely that two Dirac-Fock solutions, one for the ground state of an atom and another for an excited state of the same atom, belong to the same set of eigenfunctions when the two wave functions are individually optimized- known as the wave functions with a relaxed core- particularly for states with several open-shell configurations. This question of forming a complete set also applies to nonrelativistic Hartree-Fock wave functions

A practical way to circumvent the question of a projection operator is to generate a set of relativistic eigenfunctions from a model relativistic Hamiltonian, and use linear combinations of positive energy solutions only (including the usual bound-state solutions) to approximate true solutions. In this way, a true solution is limited to the function space spanned by positive energy solutions of a model relativistic Hamiltonian. This prescription is not equivalent to constructing a rigorous projection operator because the answer would depend on the choice of the model Hamiltonian and on the number of basis functions retained to approximate solutions. We must continue to look for a practical, but less model-dependent solution to this problem.

In principle, basis functions can be either analytic or numerical functions. The use of basis functions may bring additional benefits, taking advantage of vectorization and parallel processing in modern computers. In a generic relativistic MBPT (RMBPT), a complete set of eigenfunctions is generated from a model Hamiltonian, usually a closed-shell Dirac-Fock equation. The orbitals used to defined the unperturbed Dirac-Fock equation is then kept frozen, and the same DF equation is used to generate all other one-electron, relativistic orbitals. Then, these orbitals are used to construct wave functions for many-electron atoms and to calculate contributions from various diagrams according to the rule of MBPT. One distinct advantage of RMBPT is that it is well suited to incorporate QED correction, since both theories use Feynman-like diagrams and facilitate seeing what is included at each stage. For cases involving small number of bound electrons, a large scale MCDF calculation can match the accuracy of an RMBPT calculation. However, the MCDF values would include partial contribution from many orders of perturbations, making it difficult to compare the two theoretical methods directly.

Although RMBPT calculations account for both relativistic and correlation effects well,

the theory has two major drawbacks. First, the current version of the theory can be applied only to limited types of open shell configurations. Second, there is no guarantee of convergence, e.g., there is no guarantee that the total contribution from third-order perturbation diagrams is smaller than that from second order perturbation diagrams, and so on. RMBPT calculations for third order diagrams are so complicated that it is difficult to imagine performing a fourth order calculation even with a supercomputer in the foreseeable future. Fortunately, quantities associated with highly charged ions, such as energies, seem to converge quickly so that second order perturbation calculations exhibit remarkable agreement with experiment when direct comparisons are possible. Applications to neutral atoms or lightly charged ions, however, may require higher order diagrams that may not be easy to evaluate.

There have been attempts to build MBPT from a more advanced starting point, such as an MCHF or MCDF wave function rather than a single-configuration HF or DF wave function. Such attempts, however, have not demonstrated that they can efficiently handle arbitrary open-shell configurations. Expanding the type of open-shell configurations that an MBPT can handle is an urgent and major task to be pursued. As more accurate spectroscopic data on highly charged ions became available in the last decade, it became imperative to include QED effect in the calculations before making any serious comparison between theory and experiment. It is clear now that theoretical predictions of atomic energy levels must include correlation, relativity, QED as accurately as possible. Moreover, correlation and relativity effects are neither separable nor additive, but are coupled together. As we try to achieve better accuracy, we are likely to find that QED corrections are also coupled. For instance, radiative corrections are most effective near the nucleus and may change the shape of the wave functions there. Most current relativistic structure theories treat QED corrections as uncoupled perturbations.

QED corrections based on the hydrogen-like ions, however, must be modified to take mutual screening among all bound electrons into account.Theoretical methods to estimate this screening correction to QED corrections are beginning to emerge for comparison with limited experimental data on highly charged ions with simple electronic structures. More experimental data on He- and Li- like heavy ions are highly welcome at present. Substantial improvements are needed in theories such as the MCDF and RMBPT methods to provide definitive values of correlation and relativistic corrections for complex atoms, thus opening the way to obtain reliable estimates of QED corrections from comparisons of theoretical and high precision experimental data.

Theorists working on relativistic atomic structure theory face a golden opportunity now provided by the ever-increasing power of computers (supercomputers, workstations, massively parallel computers, etc.), by the accurate spectroscopic data on highly charged ions generated by tokamaks, powerful lasers and heavy ions accelerators, and by the

considerable experience accumulated concerning the nonrelativistic correlation problem. Already, some relativistic theoretical predictions are accurate enough to identify errant experimental data and to serve as guidelines for new experiments. There are, however, several questions to be settled because of the peculiarity of relativistic theory before we can expect precise theoretical predictions to become available for a wider class of atomic configurations. The questions discussed here primarily relate to the prediction of energy levels, but methods that provide accurate energy eigenvalues should also yield reliable expectation values other than energies, for examples. oscillator strengths, lifetimes, etc. Independent particle models (e.g. central potential model, Hartree-Fock Slater method, Hartree-Fock method) describe qualitatively the properties of many- electron atoms, molecules and ions. Independent particle model deviates quantitatively substantially from the experimental observations. It clearly demonstrates that it is indispensable to incorporate electron correlation in order to obtain accurate results. Electron correlation is defined as the difference between the exact energy for a certain Hamiltonian and the Hartree-Fock (or single configuration) energy for the same Hamiltonian operator. It is simply the correction to zero-order approach. A physical interpretation is the dynamic behaviour of the electrons, which in single configuration model move independently of each other in an average central field. Correlation introduces the fact that they actually do avoid each other in their orbits. Nonrelativistic correlations are included widely in two methods: configuration-interaction (CI) and multiconfiguration Hartree-Fock (MCHF). Tiwary and his $co-workers$[25-55] have extensively investigated the effect of correlation on the optical oscillator strengths, both the length (f_L) and velocity (f_V) forms, in alkali atoms and alkali- like ions using uncorrelated and correlated wave functions for both the initial and final states involved in the transition. For ground state configuration, all orbitals are taken from Clementi and $Roetti$[56]. Several standard computer $codes$[57-64] are available for the accurate atomic structure calculations. For low Z atoms and ions, these methods produce good results but for heavy systems they disagree with the experiment which suggest that relativistic as well as correlation effects play important role for reliable results. Accurate prediction of excitation energies, oscillator strengths, lifetime, etc., in alkali atoms and alkali-like ions, particularly for the heavier members of the group, requires high- order incorporation of both relativistic and correlation effects. We therefore start from the $Dirac$[19] Coulomb or Dirac-Coulomb- $Breit$[20] Hamiltonian. The latter is correct to the second order in the fine structure constant. The four-component one-electron equations, in the Dirac-Fock or Dirac-Fock-Breit approximation, are solved. Relativistic correlation is then incorporated by the multiconfiguration Dirac-Fock (MCDF) method. Relativistic and electron correlation effects are strongly interwined. Accurate treatment of many electron systems requires therefore going beyond the independent particle model to incorporate relativistic and correlation simultaneously on an equal footing. A variety

of techniques can be employed for the study of dynamic correlation in particle systems. The extensive practice of nonrelativistic as well as relativistic calculations, including those for alkali atoms shows that many body perturbation theory is a powerful and systematic approach. The first few terms of the perturbation series suffice for accurate calculations of the properties of highly charged ions, but the method is less suitable for neutral atoms, where higher orders of MBPT are non-negligible and sometimes even make the convenience of the perturbation expansion doubtful. The expression for higher order terms are complicated and direct perturbative studies are rarely carried out beyond second order wave functions or third order energies. It is clearly desirable to explore methods which identify important physical effects and incorporate them to all orders in perturbation theory.

One of the most interesting features of the developments of physics is when an established and successful theory is shown to be only an approximation to reality and a deeper and more encompassing theory replaces it. This has happened many times in physics: Newton theory of gravitation was replaced by Einstein general theory of relativity, nonrelativistic mechanics with relativistic mechanics, nonrelativistic classical mechanics with nonrelativistic quantum mechanics and so on. In each case the older theories remain of value but they are recognized to be only in their domain of validity. Very frequently precise measurements play a significant role in replacing a theory with a deeper or covering theory. Another exciting example is about 46 years ago when the Dirac $theory$[19] of hydrogen, which predicted the exact degeneracy of the 2 $S_{1/2}$ and 2 $P_{1/2}$ states, was shown to be very slightly incorrect by the measurement of the Lamb $shift$[65]. As tiny as the effect is, it requires the complete replacement of Dirac relativistic generalization of the Schroedinger equation. In order to explain the Lamb shift, a relativistic quantum field theory of the interacting electrons and electromagnetic fields was developed in the form of Quantum Electrodynamics (QED)[66-88].

The QED has widely applied to interpret several experimental observations of high precision. There are several theories available in the literature. All are approximate. There are main two parts of QED: self energy and vacuum polarization. We concentrate on QED effect in Li-like U^{89+} ion.

High precision experiments exhibit that only correlation, relativity and QED effects are not able to explain measurements. The effect of finite nuclear size (FNS)[89-96], though extremely small, was incorporated to interpret accurate observations. Several theoretical calculations are available for the FNS correction in atoms, molecules and ions. Recently, very high precision atomic experiments have demonstrated that the inclusion of only correlation, relativity, QED and FNS are not adequate to interpret accurate observations. The parity nonconservation (PNC) effect must be incorporated in order to explain measurements.

The parity of a system describes its behaviour under reflection through the origin. This transformation is formally equivalent to a mirror reflection in a plane through the origin plus a 180^{o} rotation about an axis perpendicular to that plane. Rotational invariance of physical system means that a parity non-conserving (PNC) system is one that exhibits a mirror asymmetry. Of the four fundamental interactions, only weak interaction is known to be parity non-conserving. The effects of weak interaction in the atomic environment leads to small mirror asymmetry such as the rotation of plane polarized light in an atomic vapour. These effects, though extremely small, are measurable because of their PNC signature. Advances in experimental techniques have enabled high precision measurement of atomic PNC phenomena. Atomic PNC effects have a Z^3 enhancement so that experiments are performed on heavy atoms: currently, atomic PNC experiments have been performed on Cs, Tl, Pb and Bi.

During the past decade, experiments to detect atomic PNC have progressed to a point where PNC amplitude can be measured with an accuracy of a few percent. To interpret such experiments in terms of the standard model of the electro-weak interaction, it is necessary to compare the measured amplitude with theoretically predicted amplitude. Predicted PNC amplitudes in heavy atoms to a accuracy of one percent is challenging exercise in many-body theory that leads beyond the independent particle model and low order perturbation theory to techniques in which important terms in perturbation theory are summed to all orders. The most precise experiments and theory have been made for Cs because the requisite atomic structure calculations can be carried out for the cesium than for the other elements.

The principal source of PNC in atoms is the exchange of Z_0 bosons between bound electrons and the atomic nucleus. The PNC interaction from Z_0 exchange consists of two parts: a dominant part in which the vector nucleon current is coupled to the axial vector electron current and a much smaller part in which the axial vector nucleon current is coupled to the vector electron current. The parity conserving part of the Z_0 exchange interaction is, of course, masked by the electron-nucleus Coulomb interaction.

Usually physicists consider measurements of the effects of PNC as a method to investigate the strength and structure of weak interaction. However, there is one other possibility i.e. investigation of a complicated quantum system or process using the PNC effects as a probe. These effects are always linear in the weak interaction matrix elements and provide more detailed information than level spacings, widths, etc. A wide range of physical effects is involved in the study of PNC[97-108] which makes it a stimulating and rewarding field. Using PNC effects one can study quantum chaos, phase transitions, nuclear fission, distribution of neutrons in nuclei, properties of weak interaction, the accuracy of both calculation and measurement to well below 1 % level, etc.

2 Theory

2.1 Correlation

Very general methods, that take into account of nonrelativistic correlation and can be used for even the most complex atoms and ions, are the configuration interaction (CI) and multiconfiguration Hartree-Fock (MCHF), which are closely related.

The basic assumption of both sets of methods is that the atom or ion is represented by an atomic or ionic state function (ASF or ISF), $\Psi(LS)$, which is a linear combination of configuration state functions (CSF), $\Phi(\alpha_i LS)$. The LS wave functions are written in the form:

$$\Psi(LS) = \sum_{i=1}^{NCSF} c_i \Phi_i(\alpha_i LS) \tag{1}$$

Each CSF is constructed as a coupled, antisymmetric sum of products of one particle functions, $\phi_{nl}(r)$, called spin-orbitals,

$$\Phi_{nl}(r) = \frac{1}{r} P_{nl}(r) Y^l_{m_l}(\theta, \varphi) \chi_{m_s} \tag{2}$$

The coefficients c_i are the eigenvectors components of the Hamiltonian matrix with typical element

$$H_{ij} = < \Phi_i | H | \Phi_j > \tag{3}$$

Φ_j are single-configuration functions constructed from one-electron functions, whose orbital and spin momenta are coupled to form the common total angular- momentum quantum numbers L and S according to a prescription denoted in (1) by α_i. We express the radial parts of the one-electron functions in analytical form as a sum of Slater-type orbitals, following Clementi and *Roetti*[56] :

$$P_{nl} = \sum_{j=1}^{k} C_{jnl} r^{I_{jnl}} e^{-\xi_{jnl} r} \tag{4}$$

The parameters in (3) can be varied to optimize the energy of any state, subject to the orthonormality conditions

$$\int_0^\infty P_{nl}(r) P_{n'l}(r) dr = \delta_{nn'} \tag{5}$$

In equation (1) and (2), there are two sets of unknown, the c_i coefficients and radial functions $P_{nl}(r)$. The difference between the CI and MCHF methods is now basically just the way the last set is obtained. In MCHF method, the variational principle is employed to derive a set of coupled integro-differential equations, one for each radial fnnctions, while coefficients are obtained by solving a secular equation, of the form

$$[H - EI]c = 0 \tag{6}$$

where the matrix **H** has the elements $H_{ij} =< \Phi_i|H|\Phi_j >$ and H is the Hamiltonian operator. These two optimizations are performed at the same time, in an iterative method usually labeled self-consistent field. In CI calculations, on the other hand, the radial functions are predetermined and only the secular equation is solved for the coefficients.

2.1.1 Many-body Perturbation Theory (MBPT)

Brueckner[10] and *Goldstone*[11] have originally developed the many-body perturbation theory for the study of the structure of many-body systems of infinite extent, in particular, infinite nuclear matters. For the first time, *Kelly*[11] introduced the MBPT into atomic physics. It is based on a second quantization form of Rayleigh-Schroedinger perturbation theory and makes extensive use of Feynman diagrams.
The Hamiltonian is split according to

$$H = H_0 + H_1 \tag{7}$$

where H_0 is a sum of one-electron operators:

$$H_0 = \sum_{i=1}^{N}(-\frac{1}{2}\nabla_i^2 + V(r_i)) \tag{8}$$

and in practice the HF potential V is used. Then (March et *al*[13])

$$H_0 = \sum_n \epsilon_n \eta_n^\dagger \eta_n \tag{9}$$

$$H_1 = \sum_{p,q,m,n} < pq|\frac{1}{r_{12}}|mn > \eta_p^\dagger \eta_q^\dagger \eta_n \eta_m - \sum_{p,m} < p|V|m > \eta_p^\dagger \eta_m \tag{10}$$

where ϵ_n are the eigenvalues of the Fock operator, $\eta^\dagger$, η creation and annihilation operators, and sums are over all states (orbitals), occupied and unoccupied in HF (denoted unexcited and excited respectively). An unoccupied unexcited state is called a hole, and an occupied excited state is called particle. Interactions such as those occurring in equation (10) may be represented by Feynman diagrams. A particle in excited state is represented by a line directed upwards, a hole in an unexcited state by a line directed downwards, and the interaction by a horizontal broken line. Diagrams which occur in equation (10) are exhibited in Fig. 1. A diagram is unlinked if it contains parts which are completely disconnected, otherwise diagrams are linked.
After carrying out a time dependent perturbation analysis, the exact wave function may be expanded as

$$\Psi = \sum_{n=0}^{\infty}{}^{L}(\frac{1}{E_0 - H_0}H_1)^n \Psi_0 \tag{11}$$

where E_0 is the appropriate eigenvalue of H_0, and superscript L indicates that only linked diagrams are included in the summation. Also

$$E = E_0 + \sum_{n=0}^{\infty}{}^{L'} < \Psi_0|H_1(\frac{1}{E_0 - H_0}H_1)^n|\Psi_0 > \tag{12}$$

where superscript L' indicates that only those linked diagrams arising from equation (10) are included.
Since the HF potential V is used

$$< a|V|b >= \sum_{m=1}^{\infty}[< am|\frac{1}{r_{12}}|bm > - < am|\frac{1}{r_{12}}|mb >] \tag{13}$$

where the sum is over the HF orbitals. The corresponding diagrams for these three interactions are shown in Fig. 2. For a, b excited, these diagrams sum to zero in the evaluation of the first order energy $E_1 =< \Psi_0|H_1|\Psi_0 >$. Only the unexcited terms remain, giving

$$E_1 = -\frac{1}{2}\sum_{m=1}^{N} < m|V|m > \tag{14}$$

and

$$E_0 + E_1 = E^{HF} \tag{15}$$

We will not discuss the details of the theory here and we refer the reader to the article by Kelly.

2.2 Relativity

Many-electron Schroedinger Hamiltonian can be written as

$$H^S = \sum_{i=1}^{N}[\frac{p_i^2}{2m} - \frac{Z(r)}{r_i}] + \sum_{i \neq j}\frac{1}{|r_i - r_j|} \tag{16}$$

This Hamiltonian does not include the relativistic effect. In 1928, *Dirac*[19] proposed a relativistic (Lorentz covariant) equation for an electron which, in the central field of a nucleus with charge Z, can be written as follows (in atomic unit):

$$H^D\psi = E\psi \tag{17}$$

where the Dirac Hamiltonian, H^D, is of the form (for one-electron system):

$$H^D = c\alpha.p + c^2\beta m - Z/r, \tag{18}$$

where
α is the Dirac matrix

$$\alpha = \begin{pmatrix} 0 & \sigma^P \\ \sigma^P & 0 \end{pmatrix} \tag{19}$$

and

β is the Dirac matrix

$$\beta = \begin{pmatrix} I & 0 \\ 0 & -I \end{pmatrix} \tag{20}$$

In equation (18) c is the velocity of light, r is the electron-nucleus distance (point nucleus is used, although the finite size of the nucleus presents no difficulties) and p is the linear momentum operator of the electron. The α and β are the Dirac 4×4 matrices, which can be written in the standard representation in terms of 2×2 Pauli matrices, σ^P, and 2×2 unit matrix, I as in equation (20).

The eigenfunctions, ψ, of equation (17) are four-component spinors and these can be chosen as eigenfunctions of the set of commuting operators: H^D, J^2, the total angular momentum squared, J_z , the projection of J on the Z-axis. The eigenvalues of these commuting operators are E, j(j + 1), m and k, respectively. The four-component eigenspinors, ψ_{nkm}, can be written as:

$$\psi_{nkm}(r,\theta,\phi) = \begin{pmatrix} r^{-1}P_{nk}(r)\chi_{km}(\theta,\phi) \\ ir^{-1}Q_{nk}(r)\chi_{-km}(\theta,\phi) \end{pmatrix} \tag{21}$$

The $r^{-1}P_{nk}$ and $r^{-1}Q_{nk}$ are the large and small radial functions and the $\chi_{km}((\theta,\phi)$, the two-component spinors. Details are given elsewhere. It is well known that Dirac theory accounts for many experimental results for one-electron system. One may, therefore, believe that the Dirac theory is the starting point for a relativistic treatment of many-electron systems and the Dirac-Coulomb Hamiltonian for many-electron system can be written as

$$H^{DC} = H^D + H^C \tag{22}$$

$$H^{DC} = \sum_{i=1}^{N}[\alpha_i.p_i + \beta_i m - \frac{Z(r)}{r_i}] + \tag{23}$$

$$\sum_{i \neq j} \frac{1}{|r_i - r_j|} \tag{24}$$

It is not possible to generalize the Dirac theory to many-electron systems. A fully Lorentz invariant Hamiltonian for many-electron systems can not be obtained in a closed form because the complete electron-electron interaction involves, in addition to the instantaneous Coulomb interaction (r_{ij}^{-1}, which is not Lorentz invariant), the exchange of virtual photons between interacting electrons. However, *Breit*[20] proposed H^{Br} as a correction to the Coulomb interaction, r_{ij}^{-1} for two electrons as:

$$H^{Br} = -\frac{1}{2}[\sum_{i=1}^{N} \frac{\alpha_i.\alpha_j}{r_{ij}} + \frac{\alpha_i.r_{ij}.\alpha_j.r_{ij}}{r_{ij}^3}] \tag{25}$$

The Dirac-Coulomb-Breit Hamiltonian H^{DCB} can be written as:

$$H^{DCB} = H^D + H^C + H^B \tag{26}$$

H^{Br} takes into account the magnetic and retardation terms and is of the order of $(Z/c)^2$, relative to the Coulomb interaction. Thus, it should be used as the first-order perturbation to the zeroth order Hamiltonian. The difficulty with this Hamiltonian is that the Breit interaction, which is a correlation to the nonrelativistic Coulomb interaction r_{ij}^{-1}, represents only the first order relativistic correlation. In the language of Feynman diagrams, it represents the exchange of only one virtual photon between the two interacting electrons. In principle, there are higher order corrections corresponding to the exchange of two, three, etc., virtual photons. Much work is still needed to calculate these higher-order corrections to the Breit interaction.

Relativistic effects may be added to the Hamiltonian in the form of the Breit-Pauli interaction, of which we include the spin-orbit, spin-other-spin, spin-spin, mass correction, and one-body Darwin terms. The Breit-Pauli Hamiltonian can be written as:

$$H^{BP} = H_{NR} + H_R \tag{27}$$

where H_{NR} is nonrelativistic Coulomb Hamiltonian and

$$H_R = H_{so} + H_m + H_{D1} + H_{soo} + H_{ss} + H_{oo} + H_{D2} + H_{ssc} \tag{28}$$

is the relativistic correction.

$$H_{so} = \frac{\alpha^2 Z}{2} \sum_{i=1}^{N} \frac{1}{r_i^3}(l_i.s_i) \tag{29}$$

represents the one-body spin-orbit interaction of each electron magnetic moment with the magnetic field arising from the electron own motion in the Coulomb field of the nucleus;

$$H_m = -\frac{\alpha^2}{8} \sum_{i=1}^{N} \nabla_i^4 \tag{30}$$

is the relativistic mass correction;

$$H_{D1} = -\frac{\alpha^2 Z}{8} \sum_{i=1}^{N} \nabla_i^2(\frac{1}{r_i}) \tag{31}$$

is the one-body Darwin term; the relativistic correction to the potential energy;

$$H_{soo} = -\frac{\alpha^2}{2} \sum_{i \neq j} (\frac{r_{ij}}{r_{ij}^3} \times p_i).(s_i + 2s_j) \tag{32}$$

represents the spin-other-orbit interaction and is made up of two parts. The first one containing the factor s is the spin orbit coupling of electron i in the Coulomb field of the electron j. The second, with the factor 2s comes from the interaction of the spin magnetic moment of electron j with the orbital current i;

$$H_{ss} = \alpha^2 \sum_{i \neq j} \frac{1}{r_{ij}^3}[(s_i.s_j) - 3\frac{(s_i.r_{ij})(s_j.r_{ij})}{r_{ij}^2}] \tag{33}$$

is the ordinary dipole interaction of the spin magnetic moments of two electrons;

$$H_{oo} = -\frac{\alpha^2}{2}\sum_{i\neq j}[\frac{p_i.p_j}{r_{ij}} + \frac{r_{ij}(r_{ij}.p_i).p_j}{r_{ij}^3}] \tag{34}$$

is the orbit-orbit interaction;

$$H_{D2} = \frac{\alpha^2}{4}\sum_{i\neq j}\nabla_i^2(\frac{1}{r_i}) \tag{35}$$

is the two-body Darwin term; the relativistic correction to the potential energy;

$$H_{ssc} = -\frac{8\pi\alpha^2}{3}\sum_{i\neq j}(s_i.s_j)\delta(r_i - r_j) \tag{36}$$

is the electron spin-contact term. Some of the terms of Breit-Pauli Hamiltonian split LS states into J-dependent levels and some of them affect the overall energy. The expansion (1) is then replaced by

$$\Psi(J) = \sum_i c_i\Phi_i(LSJ) \tag{37}$$

where the summation now includes single-configuration with different L and S (which can couple to form a common J value). The matrix which is diagonalized to give the eigenenergies and eigenvectors components a_i now contain the Breit-Pauli operators as well as the previous non-relativistic terms in the Hamiltonian.

2.3 Basic Theory of Quantum Electrodynamic (QED)

Quantum electrodynamic corrections are the radiative corrections commonly known as the Lamb *Shift*[65]. The Lamb shift may be written as a sum over terms representing different physical effects:

$$E_{LS} = \delta E_{SE} + \delta E_{VP} + \delta E_{FNS} + \delta E_{HO} + \delta E_{RC} \tag{38}$$

with: SE, electron self energy correction; VP, vacuum polarization correction; FNS, correction due to the finite nuclear size; HO, higher order corrections due to two virtual photons processes; RC, relativistic corrections (relativistic recoil and relativistic reduced mass).

From the point of view of field theory, the vacuum polarization correction is the result of the process in which the photon that mediates the Coulomb interaction between the bound electron and the nucleus produces a virtual electron-positron pair in the vacuum. The corresponding Feynman diagram is given in Fig. 4. The diagram gives a correction to the Coulomb potential V(r) known as the *Uehling*[67] potential $\delta V(r)$:

$$V(r) \rightarrow V(r) + \delta V(r) \tag{39}$$

In the Coulomb field of a nucleus of charge Ze, $\delta V(r)$ is given by

$$\delta V(r) = -\frac{\alpha}{\pi}(Z\alpha)f(r/\lambda_e)m_ec^2 \tag{40}$$

where

$$f(r/\lambda_e) = \frac{\lambda_e}{3r}\int_1^\infty dt(t^2-1)^{1/2}(2t^{-2}+t^{-4})e^{-2tr/\lambda_e} \tag{41}$$

The range of the Ueling potential is exhibited by the asymptotic form for $r >> \lambda_e$

$$f(r/\lambda_e) \sim -\frac{\pi^{1/2}}{4}(\frac{\lambda_e}{r})^{5/2}e^{\frac{-2r}{\lambda_e}} \tag{42}$$

The range of δV is short on the atomic scale, so the energy shift is proportional to the bound electron wave function at the origin, to lowest order in $Z\alpha$:

$$\begin{aligned}\Delta E_U =< \delta V >= \frac{\alpha}{\pi}\frac{(Z\alpha)^4}{n^3}G_n(Z\alpha)m_ec^2 \\ \approx -\frac{\alpha}{\pi}(Z\alpha)|\psi(0)|^2\int d^3r f(r/\lambda_e)m_ec^2\end{aligned} \tag{43}$$

In (43), the function $G_n(Z\alpha)$ gives the exact expectation value of δV calculated with Dirac wave functions. For small Z, we have

$$G_n(Z\alpha) \sim \begin{cases} -\frac{4}{15} & s \;\; states \\ 0 & p,d,.... \;\; states \end{cases} \tag{44}$$

The self energy is the dominant QED correction in ordinary atoms and ions. This is in contrast to muonic atoms where the vacuum polarization dominates. The first self energy calculation was done by *Bethe*[68] in 1947 based on the nonrelativistic formulation of radiation theory, including mass normalization. The expression he evaluated is :

$$\begin{aligned}\Delta E_{SE}^{Bethe} = \frac{\alpha}{4\pi^2c^2}\sum_{\lambda=1}^{2}\int d^3k k^{-1} < n|\hat{\epsilon}_\lambda.\vec{v}\sum_i\frac{|i><i|}{E_n - E_i - k}\hat{\epsilon}_\lambda.\vec{v}|n > \\ +\frac{1}{2}\delta m_0 < v^2 >\end{aligned} \tag{45}$$

$$\Delta E_{SE}^2 = \frac{\alpha}{\pi}\frac{(Z\alpha)^4}{n^3}F_n(Z\alpha)m_ec^2 \tag{46}$$

$F_n(Z)$ is approximately $4/3ln(Z\alpha)^{-2} + C_n$

$$H^{Furry} = \int d^3(r)\psi^\dagger(r)[\alpha.p + \beta m - \frac{Z\alpha}{r} + U(r)]\psi(r) \tag{47}$$

$$\psi(x) = \sum_{n^+} b_n\phi_n(\vec{x})e^{-iE_nt} + \sum_{n^-} d_n^*\phi_n(\vec{x})e^{-iE_nt} \tag{48}$$

$$[-i\vec{\alpha}.\vec{v} + V(\vec{x}) + \beta - E_n]\phi_n(\vec{x}) = 0 \tag{49}$$

The creation and destruction operators obey the usual Fermi anticommutation rules. Interaction of the electromagnetic current of the electron-positron field with the radiation field is provided by the interaction Hamiltonian density:

$$H_I(x) = -1/2e[\psi(x)\gamma^{mu}, \psi(x)]A_\mu(x) - 1/2\delta m[\psi(x), \psi(x)] \tag{50}$$

where -e is the electron charge and A_μ is the vector potential of the radiation field. The second term in (50) is the mass renormalization counter term. Energy level shifts are calculated in a perturbation expansion in H_I by applying the Gell-Mann and *Low*[71] theorems in the symmetric form discussed by *Sucher*[76]

$$\Delta E_n = \lim_{\epsilon \to 0} \frac{i\epsilon}{2} \frac{\frac{\partial}{\partial \lambda} < n|S_{\epsilon,\lambda}|n >}{< n|S_{\epsilon,\lambda}|n >} \tag{51}$$

where

$$S_{\epsilon,\lambda} = \sum_{j=0}^{\infty} S^j_{\epsilon,\lambda} \tag{52}$$

and where

$$S^j_{\epsilon,\lambda} = \frac{(-i\lambda)^j}{j!} \int d^4x_j ..... \int d^4x_1 e^{\epsilon|t_j| - .... - \epsilon|t_1|} \times T[H_I(x_j) .... H_I(x_1)] \tag{53}$$

$$|n >= \sum_{i_1 .... i_k} c_{i1} ... c_{ik} b^*_{i1} ... b^*_{ik} |0 > \tag{54}$$

$$S_F(x_2, x_1) = \begin{cases} \sum_{n+} \phi_n(\vec{x}_2)\phi_n(\vec{x}_1)e^{-iE_n(t_2-t_1)} & t2 > t1 \\ -\sum_{n-} \phi_n(\vec{x}_2)\phi_n(\vec{x}_1)e^{-iE_n(t_2-t_1)} & t2 < t1 \end{cases} \tag{55}$$

or

$$S_F(x_2, x_1) = \frac{1}{2\pi i} \int_{C_F} dz \sum_n \frac{\phi_n(\vec{x}_2)\phi_n(\vec{x}_1)}{E_n - z} e^{-iz(t_2-t_1)} \tag{56}$$

where C_F denotes the *Feynman*[74] contour. The lowest order diagrams for the QED correction to the energy level are shown in Fig. 5.

Wichmann and *Kroll*[72-73] have examined the complete vacuum polarization and have shown that the effect of correction to the Uehling potential included in the exact result is very small in ordinary atoms over a wide range of Z. In muonic atoms, on the other hand, this correction is of measurable magnitude.

2.4 Finite Nuclear Size (FNS)

Although, the nucleus is frequently taken to be a point source for an electron field, whence

$$V_{nucl} = -\frac{Ze^2}{r} \tag{57}$$

is the potential energy of interaction between an electron and nucleus, other models the account for the finite size of the nuclear charge distribution are commonly employed for high precision calculations and

$$V_{nucl} = -\frac{Z(r)e^2}{r} \tag{58}$$

Possible models for the charge distribution in the nucleus include a hollow shell charge distribution with radius R_s

$$\rho_s(r) = \frac{Ze}{4\pi R_s^2} \delta(r - R_s), \tag{59}$$

a spherically symmetric uniform charge distribution with surface radius R_u

$$\rho_u(r) = \frac{Ze}{4/3\pi R_u^3} \theta(R_u - r), \tag{60}$$

and the Fermi model

$$\rho_f(r) = \frac{\rho_0}{1 + e^{\frac{r-c}{a}}}. \tag{61}$$

For the binding energy, the dependence on the model is small provided the root mean square (rms) radius of the charge distribution

$$R = [\frac{1}{Ze} \int dr r^2 \rho(r)]^{1/2} \tag{62}$$

is fixed to a particular value.

2.5 Basic Theory of Parity Non-conservation (PNC)

The dominant part of the PNC interaction can be expressed as a correction of the atomic Hamiltonian:

$$H^{PNC} = G_F Q_W \frac{1}{2\sqrt{2}} \rho(r) \gamma_5 \tag{63}$$

where $G_F = 2.22 \times 10^{-14}$ au gives the small size of the interaction, $\rho(r)$ is the nuclear density, Q_W is the weak charge and given by

$$Q_W = -N + Z(1 - 4Sin^2\theta_W) \tag{64}$$

where N and Z are the number of neutrons and electrons respectively. $Sin^2\theta_W$ is the fundamental parameter for the standard electro-weak *model*[97-99] and γ_5 is the matrix

$$\gamma_5 = \begin{pmatrix} 0 & 1 \\ 1 & 0 \end{pmatrix} \tag{65}$$

When this matrix acts on a relativistic Dirac two component spinor it exchanges the top and the bottom components so that the resulting orbital has the opposite normal parity of the unperturbed orbital. This gives the PNC nature of the atomic weak interaction Hamiltonian.

The presence of atomic PNC weak interaction means that quantities which are normally forbidden can now occur. For example: Cs $6s \to 7s$ E1 transition is parity forbidden. In the presence of PNC interaction the orbitals become parity mixed so that there is then a non-zero matrix element or amplitude for this transition due to the opposite parity of the admixture.

$$< 7s^-|r|6s^- >=< 7s^{PNC}|r|6s > + < 7s|r|6s^{PNC} > \tag{66}$$

where - denotes a parity mixed orbital. The $6s \rightarrow 7s$ transition amplitude, which is proportional to Q_W, can be measured experimentally. If the value of Q_W can be extracted then a value for the $Sin^2\theta_W$ can be obtained. However, in order to extract Q_W it is necessary to have a value for the PNC E1 transition matrix element. These have to be calculated separately and this is the task of atomic PNC theory. The most accurate PNC measurements have been performed on Cs and this is a single valence system the theory is relatively easy.

3 Results and discussion

Table 1 displays the Hartree-Fock (HF) and configuration-interaction (CI) J- dependent and -independent optical oscillator strengths of the inner-shell excitation $1s^22s^22p^63s\ ^2S^e_J \rightarrow 1s^22s^22p^53s^2\ ^2P^o_J$ transition, which leads to autoionization, of both length (f_L) and velocity (f_V) forms, in Fe^{15+} ion of the sodium isoelectronic sequence. It is clear from the Table that there is disagreement between the HF (f_L) and (f_V) which suggests that the correlation must be included. The CI (f_L) and (f_V) is in better agreement but the discrepancy remains which indicates the importance of the relativity. The relativity has been included in the calculation via Breit-Pauli Hamiltonian. The Table exhibits the J-dependent oscillator strengths and better agreement has been achieved. In order to see the general trend of the oscillator strengths in the sodium isoelectronic sequence, we have plotted f_L as a function of $\frac{1}{Z}$ in Fig. 3.

Tables 2-4 show the HF and CI optical oscillator strengths of the inner-shell excitation $1s^22s^22p^63s^23p^63d\ ^2D^e \rightarrow 1s^22s^22p^63s^23p^53d^2\ ^2P^o$, $^2D^o$ and $^2F^o$ transitions, which leads to autoionization, in Sc^{2+}, Ti^{3+} and V^{4+} ions of the potassium isoelectronic sequence. It is clear from Tables 2-4 that the HF (f_L) and (f_V) disagree with each other by about a factor of two. This disagreement indicates that the HF description is not adequate. It is indispensable to incorporate the correlation. The CI (f_L) and (f_V) has good agreement which demonstrates the importance of the correlation. Table 5 gives the resonance excitation energy in Li-like U^{89+} ion. The Table displays the effects of relativity, correlation, and quantum electrodynamic. The agreement between the experiment and theory is good. However, the discrepancy exists which suggests to include other physical effects, e.g., finite nuclear size (FNS), parity nonconservation (PNC). Table 6 presents the self energy in Li-like U^{89+} ion showing the effect of the nuclear size.

Blundell et al^{105} have extensively investigated and reviewed the PNC effects (see references therein). Table 7 presents the PNC amplitude in Cs. Several calculations have been carried out. Overall, there is reasonably good agreement between the theoretical predictions and experimental observations. Table 8 gives the fundamental parameter in the standard model $Sin^2\theta_W$. The atomic physics gives good value of the $Sin^2\theta_W$ compare

to the world average value which indicates that the atomic physics is capable of providing information about the weak interaction. Table 9 gives the ionization energy of Cs with the correction of PNC. It demonstrates that the PNC plays an important role in order to obtain the accurate results.

4 Conclusions and future directions

The high-precision investigation of the effects of correlation, relativity, QED, FNS and PNC by experiments provides very sensitive test of the theoretical methods. Such stringent tests are especially important as the general problem of QED and PNC theories is extremely difficult and has not been solved completely until now. Only correlation and relativity have been treated on an equal footing in the MCDF and RMBPT. The MCDF and RMBPT results are in excellent agreement with experiments which have not included the QED and PNC effects. Most experiments do not isolate these physical effects. No experiment has separated all effects. More precise experimental investigation would be desirable. Most of the theories , for examples, MCDF and RMBPT, include correlation and relativity effects simultaneously in a unified manner. However, these theories do not explain the Lamb shift which suggest to develop new theoretical methods. Several theoretical techniques are available in the literature for the calculations of QED, FNS and PNC effects independently. There is disagreement between high precision experiment and high precision theory. It is probably because that no theoretical method incorporates all effects simultaneously on an equal footing. At present, we do not have a comprehensive and practical theory that accounts all these physical effects simultaneously.

A hybrid theory, which combines the effectiveness of the MCDF method in dealing with the most obvious addition of more subtle correlation through the MBPT, provides our best hope for a unified theory that accounts for all effects simultaneously and systematically. Another direction which can exploit the close relation between the RMBPT and QED and the productive cross fertilization of these two may be capable of yielding excellent results of accuracy well below 1% level.

In short, our knowledge of high-precision electronic structure of atoms and ions, particularly for heavy atoms and ions, is by no means complete. Comprehensive and painstaking work needs to be done and the field will continue to grow, develop and flourish. The future holds many challenges for both experiment and theory.

Acknowledgments

The author would like to thank Professor Abdus Salam, the International Atomic Energy Agency and UNESCO, for hospitality at the International Centre for Theoretical Physics, Trieste, Italy and Swedish Agency for Research Cooperation with Developing Countries (SAREC) for financial support during his visit at the ICTP under the Associateship scheme. He wishes to express his thanks to BRAB University, India, for leave and also to UGC, New Delhi, for Major Research Project.

References

1. N. Bohr, Phil Mag. 26, 1 (1913).
2. E. Rutherford, Phil. Mag. 21, 669 (1911).
3. M. Planck, Ann. Physik, 4, 553 (1901).
4. E. Schroedinger, Ann. Phys. Lpz 79, 361 (1926).
5. L. de Broglie, Ann. d. Phys. 3, 22 (1925), Thesis, Paris, 1924.
6. W. Heisenberg, Z. Physik 33, 879 (1925).
7. D. R. Hartree, Proc. Camb. Phil. 24, 89 (1928).
   The Calculation of Atomic structures, New York:Wiley, 1957.
8. V. Fock, Z. Phys. 61, 126 (1930).
9. J. C. Slater, Phys. Rev. 35, 210 (1930),
   Quantum Theory of Atomic Structure, Vol I and Vol II,
   McGraw-Hill, New York, 1960.
10. K. A. Brueckner, Phys. Rev. 97, 1353 (1955).
11. J. Goldstone, Proc. Roy. Soc. A 239, 267 (1957).
12. H. P. Kelly, Phys. Rev. 131, 684 (1963), 136, 896 (1964), 144, 39 (1966).
14. N. H. March, W. H. Young and S. Sampanthar, The Many-body Problem in
    Quantum Mechanics, Cambridge University Press, 1967.
13. A Sommerfeld, Ann. Phys. Lpz 51, 1 (1916).
15. A. Einstein, Ann. Physik, 17, 891 (1905).
15. E. U. Condon and G. H. Shortley, Theory of Atomic Structure,
    Cambridge University Press, 1935.
17. E. U. Condon and H. Odabasi, Atomic Structure,
    Cambridge University Press, 1980.
18. C. G. Darwin, Phil. Mag. 39, 537 (1920).
19. P. A. M. Dirac, Proc. Roy. Soc. (London), A 117, 610 (1928),
    118, 351 (1928), The Principle of Quantum Mechanics, Oxford University Press, 1958.
20. G. Breit, Phys. Rev. 34, 553 (1929), 36, 383 (1930).
21. B. Swirles, Proc. Roy. Soc. A 152, 625 (1935).
22. G. E. Brown and D. G. Ravenhall, Proc. Roy. Soc. 208, 552 (1951).
23. E. A. Hylleraas, Z. Physik 48, 469 (1928).
24. M. H. Mittleman, Phys. Rev. A 24, 1167 (1981).
25. S. N. Tiwary, Chem. Phys. Lett. 93, 47 (1982).
26. A. Hibbert, A. E. Kingston and S. N. Tiwary, J. Phys. B: 15, L643 (1982).
27. S. N. Tiwary, Chem. Phys. Lett. 96, 333 (1983).
28. S. N. Tiwary, A. E. Kingston and A. Hibbert, J. Phys. B: 16, 2457 (1983).
29. S. N. Tiwary, Astrophys. Journal 269, 803 (1983).
30. S. N. Tiwary, Astrophys. Journal 272, 781 (1983).

31. S. N. Tiwary, P. G. Burke and A. E. Kingston, ICPEAC, Berlin, West Germany, 1983.
32. S. N. Tiwary, Proc. Ind. Acad. Sci. 93, 1345 (1984).
33. S. N. Tiwary, ICTP, Trieste, Italy, Preprint, (1985).
34. S. N. Tiwary, ICTP, Trieste, Italy, Preprint, (1986).
35. S. N. Tiwary, Invited Talk, Book-World Book Publisher, New York, 1987.
36. A. E. Kingston, A. Hibbert and S. N. Tiwary, J. Phys. B: 20, 3907 (1987).
37. S. N. Tiwary,A. P. Singh, D. D. Singh and R. J. Sharma, Can. J. Phys. 66, 405(1988).
38. S. N. Tiwary and G. Dujardin, Symposium on Auger Process, Paris, 1989.
39. S. N. Tiwary, ICPEAC, New York, USA (1989).
40. S. N. Tiwary, ICAP-12, Ann Arbor, Michigan, 1990, USA.
41. S. N. Tiwary, Praman-J. Phys. 35, 89 (1990).
42. S. N. Tiwary, ICTP, Trieste, Italy, preprint (1990).
43. S. N. Tiwary, Fizika, 22, 577 (1990).
44. S. N. Tiwary and P. Kumar, Acta Phys. Pol. 80, 23 (1991).
45. S. N. Tiwary, Int. J. Theor. Phys. 30, 825 (1991).
46. S. N. Tiwary, Fizika 23, 27 (1991).
47. S. N. Tiwary, Nuovo Cimento D, 13, 1073 (1991).
48. S. N. Tiwary, Fizika, 1, 181 (1992).
49. S. N. Tiwary and D. D. Singh, Nuovo Cimento D 14, 739 (1992).
50. S. N. Tiwary, M. Kumar, D. D. Singh and P. Kumar, Nuovo Cimento D 15, 77 (1993).
51. S. N. Tiwary, P. Kandpal and A. Kumar, Nuovo Cimento D 15, 1181 (1993).
52. S. N. Tiwary and P. Kandpal, Nuovo Cimento D 16, 339 (1994).
53. S. N. Tiwary, Conf. on Heavy Ion Collision, BHU, Banaras, 1994.
54. S. N. Tiwary and P. Kumar, ICTP, Trieste, Italy, Preprint, 1994.
55. S. N. Tiwary, LAMP, ICTP, Trieste, Italy, 1994.
56. E. Clementi and C. Roetti, At. Data Nucl. Data Tables **14**, 177 (1974).
57. A. Hibbert, Comput. Phys. Commun. **9**, 141 (1975).
58. R. Glass and A. Hibbert, Comput. Phys. Commun. **16**, 19 (1978).
59. C. Froese Fischer, Comput Phys. Commun. **64**, 369 (1991),
The Hartree-Fock Method for Atoms, John Wiley, NY, 1977.
60. W. Eissner, M. Jones and H. Nussbaumer, Comput. Phys. Commun. **8**, 230 (1974).
61. R. D. Cowan, The Theory of Atomic Structure and Spectra,
Univ. California Press, Berkeley, 1981.
62. J. P. Desclaux, Comput. Phys. Commun. **9**, 31 (1975).
63. I. P. Grant, B. J. Mckenzie and P. H. Norrington,
Comput. Phys. Commun. **21**, 207 (1980).
64. K. G. Dyall, I. P. Grant, E. P. Plummer, C. T. Johnson and F. A. Parpia,
Comput. Phys. Commun. **55**, 425 (1989).

65. W. E. Lamb and R. C. Retherford, Phys. Rev. 72, 241 (1947).
66. R. Serber, Phys. Rev. **48**, 49 (1935).
67. E. A. Uehling, Phys. Rev. **48**, 55 (1935).
68. H. A. Bethe, Phys. Rev. **72**, 339 (1947).
69. H. A. Bethe and E. E. Salpeter, Quantum Mechanics of One- and Two-
Electron Atoms, Springer-Verlag, Berlin, 1957.
70. W. H. Furry, Phys. Rev. 81, 115 (1951).
71. M. Gell-Mann and F. Low, Phys. Rev. 84, 350 (1951).
72. E. H. Wichmann and N. M. Kroll, Phys. Rev. **96**, 232 (1954).
73. E. H. Wichmann and N. M. Kroll, Phys. Rev. **101**, 843 (1956).
74. R. P. Feynman, Quantum Electrodynamics, Benjamin-Cummings, 1962.
75. I. Lindgren and J. Morrison, Atomic Many-Body Theory,
2nd Edition Springer-Verlag, 1986.
76. J. Sucher, Relativistic, Quantum Electrodynamics and Weak Interactions
Effects in Atoms, eds. W. R. Johnson, P. J. Mohr and J. Sucher,
AIP Conference Proceedings, 1989.
77. J. Sapirstein and D. R. Yennie, Quantum Electrodynamics, edited by
T. Kinoshita, World Scientific, 1990.
78. H. Gould, Physica Scripta, T46, 61 (1993).
79. P. von Bretano, D. Platte, D. Budelsky, L. Kremer, H. J. Pross
and F. Scheuer, Physica Scripta, T46, 162 (1993).
80. J. P. Briand, Physica Scripta, T46, 157 (1993).
81. S. A. Blundell, Physica Scripta, T46, 144 (1993).
82. G. Soff, Physica Scripta, T46, 115 (1993).
83. G. W. F. Drake, Physica Scripta, T46, 116 (1993).
84. H. Persson, I. Lindgren and S. Salomonson, Physica Scripta, T46, 125 (1993).
85. P. J. Mohr, Physica Scripta, T46, 44 (1993).
86. T. Zhang and G. W. F. Drake, J. Phys. B:, 27, L311 (1994).
87. H. M. Quiney and I. P. Grant, J. Phys. B:, 27, L299 (1994).
88. I. Lindgren, Phys. Rep. 242, 269 (1994).
89. V. M. Shabaev, J. Phys. B: 26, 1103 (1993).
90. E. C. Seltzer, Phys. Rev. 188, 1916 (1969).
91. P. J. Mohr, At. Data Nucl. Data Tables 29, 453 (1983).
92. W. R. Johnson and G. Soff, At. Data Nucl. Data Tables 33, 405 (1985).
93. S. A. Blundell, W. R. Johnson and J. Sapirstein, Phys. Rev. A 41, 1698 (1990).
94. K. T. Cheng, W. R. Johnson and J. Sapirstein, Phys. Rev. Lett, 66, 2960 (1991).
95. T. Franosch and G. Soff, Z. Phys. D 18, 219 (1991).
96. I. B. Sobornov, Phys. Lett. A 189, 72 (1994).

97. A. Salam, Elementary Particle Physics, ed. Svartholm, Stockholm, 1968.
98. S. Weinberg, Phys. Rev. Lett. 19, 1264 (1967).
98. S. L. Glashow, Phys. Rev. D 2, 1285 (1970).
100. M. C. Noecker, B. P. Masterson, and C. E. Wieman, Phys. Rev. Lett. 61, 310 (1988).
101. P. G. H. Sandars, J. Phys. B: 10, 2983 (1977).
102. V. A. Dzuba, V. V. Flambaum and O. P. Sushkov, Phys. Lett. A 140, 493 (1989).
103. M. A. Bouchiat and C. C. Bouchiat, Phys. Lett. B 48, 111 (1974).
104. S. A. Blundell, A. C. Hartley, Z. Liu, A. M. Martensson-Pendrill and J. Sapirstein, Theor. Chem. Acta 80, 257 (1991).
105. S. A. Blundell, J. Sapirstein and W. R. Johnson, Phys. Rev. D 45, 1602 (1992).
106. I. B. Khriplovich, Parity Nonconservation in Atomic Phenomena, Gordon and Breach, Philadelphia, 1991.
107. B. W Lynn and P. G. H. Sandars, J. Phys. B: 27, 1469 (1994).
108. R. J. Rafac, C. E. Tanner, A. E. Livingston and K. W. Kukla, Phys. Rev. A 50, R1976 (1994).

Table 1.

J-independent and -dependent oscillator strengths of
$1s^2 2s^2 2p^6 3s\ {}^2S^e_j \rightarrow 1s^2 2s^2 2p^5 3s^2\ {}^2P^o_j$
in the sodium isoelectronic sequence

	present results		other results		present results			
function	f_L	f_V	f_L	f_V	$2J+1$	$2J'+1$	f_L	f_V
HF	0.064	0.060			2	2	0.022	0.019
					2	4	0.043	0.040
CI	0.084	0.087	0.087	0.084	2	2	0.031	0.028
					2	4	0.059	0.056

Table 2.

Optical oscillator strengths of $1s^2 2s^2 2p^6 3s^2 3p^6 3d\ {}^2D^e \rightarrow 1s^2 2s^2 2p^6 3s^2 3p^5 3d^2\ {}^2P^o$
in the potassium isoelectronic sequence

	Sc^{2+}		Ti^{3+}		V^{4+}	
function	f_L	f_V	f_L	f_V	f_L	f_V
HF	1.18	0.63	**1.12**	**0.59**	**1.03**	**0.54**
CI	0.71	0.78	0.65	**0.72**	**0.78**	**0.86**

Table 3.

Optical oscillator strengths of $1s^22s^22p^63s^23p^63d\ ^2D^e \rightarrow 1s^22s^22p^63s^23p^53d^2\ ^2D^o$ in the potassium isoelectronic sequence

	Sc^{2+}		Ti^{3+}		V^{4+}	
function	f_L	f_V	f_L	f_V	f_L	f_V
HF	2.46	1.24	**2.31**	**1.15**	**2.13**	**1.06**
CI	1.40	1.16	**0.56**	**0.44**	**1.82**	**1.55**

Table 4.

Optical oscillator strengths of $1s^22s^22p^63s^23p^63d\ ^2D^e \rightarrow 1s^22s^22p^63s^23p^53d^2\ ^2F^o$ in the potassium isoelectronic sequence

	Sc^{2+}		Ti^{3+}		V^{4+}	
function	f_L	f_V	f_L	f_V	f_L	f_V
HF	1.80	1.14	**1.69**	**1.06**	**1.56**	**0.98**
CI	0.64	0.64	1.21	**1.16**	**0.46**	**0.44**

Table 5.

Resonance excitation $1s^22s\ ^2S_{1/2} \rightarrow 1s^22p\ ^2P_{1/2}$ transition energy (in eV) of Li-like U^{89+} ion

Dirac-Fock, without Breit	**286.54**
Breit interaction	**36.44**
Correlation (RMBPT-DF)	**-0.73**
Hydrogenic self energy	**-43.96**
Self energy screening	**2.38**
Total screened QED corrections	**-41.57**
Total DF + RMBPT	**280.68**
Experiment	**280.59 + 0.10**

Table 6.

Self energy (in eV) of the 2 $S_{1/2}$ and 2 $P_{1/2}$ states in Li-like U^{89+} ion

Physical effects	**2** $S_{1/2}$	**2** $S_{1/2}$	**2**$P_{1/2}$	**2**$P_{1/2}$
Hydrogenic, point nucleus	66.38(7)[a]	66.295[b]	9.70(7)[a]	9.625[b]
Effect of nuclear size	−0.87(3)[a]	−0.90(6)[c]	−0.07(2)[a]	−0.10(5)[c]
Electronic screening, direct	−2.77(3)[a]	−2.75(2)[c]	−0.99(3)[a]	−0.97(2)[c]
Electronic screening, exchange	0.21(5)[a]		0.04(4)[a]	
Total self energy	**62.95(8)**		**8.68(8)**	

a: Persson, Lindgren and *Salomonson*[84]

b: *Mohr*[85]

c: *Blundell*[81]

Table 7.

$Cs \quad 6s \rightarrow 7s$ **PNC E_1 transition amplitude**

$(\times 10^{-11} ie a_0(-Q_W/N))$

Dzuba et al	**0.91** (1 ± 0.01)
Hartley and Sandars	**0.904** (1 ± 0.02)
Hartley et al	**0.933** (1 ± 0.04)
Johnson et al	**0.951** (1 ± 0.05)
Bouchiat and Piketty	**0.935** $(1 \pm 0.02 \pm 0.03)$

Table 8.

Fundamental parameter in the standard model $Sin^2\theta_W$

Atomic physics	$0.226 \pm 0.007(experiment) \pm 0.004(theory)$
World average	$0.2264 \pm 0.0054(experiment)$

Table 9.

Ionization energy (in atomic unit) of Cs

State	ϵ	$\delta\epsilon$	Sum	Experiment
6 $S_{1/2}$	**0.12737**	**0.01521**	**0.14257**	**0.14310**
6 $P_{1/2}$	**0.08562**	**0.00636**	**0.09198**	**0.09217**
6 $P_{3/2}$	**0.08379**	**0.00572**	**0.08951**	**0.08964**

FIGURE CAPTIONS

Fig.1 Many–body perturbation theory diagrams. (a) $\langle pq|1/r_{12}|mn\rangle$ with ϕ_m, ϕ_p, ϕ_q excited, ϕ_n unexcited; (b) $-\langle q|V|p\rangle$, (c) $\langle pq|1/r_{12}|pq\rangle$, (d) $\langle pq|1/r_{12}|qp\rangle$.

Fig.2 Many–body perturbation theory diagrams which sum to zero when V is the Hartree–Fock potential.

Fig.3 Theoretical oscillator strengths f_l as a function of 1/Z for the excitation $1s^22s^22p^63s\ ^2S^e_j \rightarrow 1s^22s^22p^53s^2\ ^2P^o_{j'}$ in the sodium isoelectronic sequence.

Curve 1, Hartree-Fock (HF);
Curve 2, HF with relativistic effect;
Curve 3, Configuration interaction (CI);
Curve 4, CI with relativistic effect.

Fig.4 Feynman diagram for the lowest-order vacuum polarization correction for a bound electron.

Fig.5 Feynman diagram for the lowest-order (a) vacuum polarization correction to bound electron energy levels and (b) self energy.

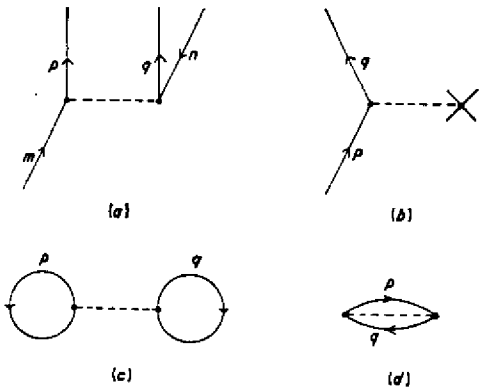

Fig.1

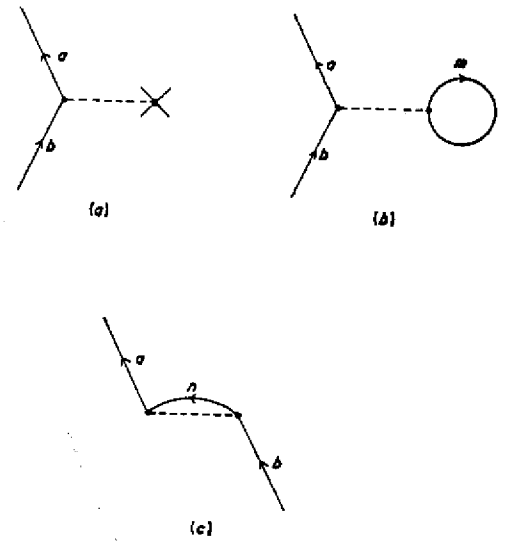

Fig.2

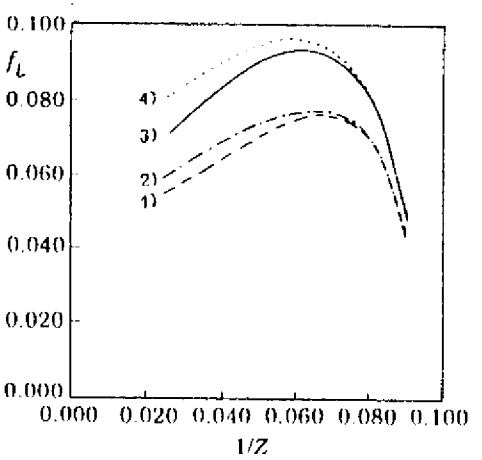

Fig.3

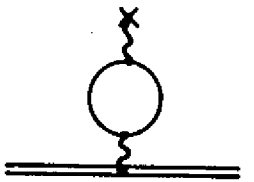

Fig.4

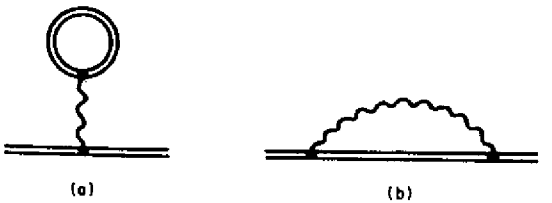

Fig.5